Chapter 8

Lipid monolayers supported by TPM microemulsions

This chapter is based on H. C. Frijters, 'Directed self-assembly of tetrahedral particles', Bachelor thesis (2015); R. W. Verweij, 'Using polymerizable microemulsions for reconfigurable colloidal clusters', Master thesis (2016); and G. L. van de Stolpe, 'The mobility of micron-sized TPM clusters', Bachelor thesis (2017).

Abstract

Supported lipid membranes are important for studying fundamental lipid membrane processes as well as for biotechnological applications. Here, we investigate microemulsions from TPM (3-(trimethoxysilyl)propyl methacrylate) as a platform for lipid monolayers. TPM droplets can be produced with a narrow size distribution, thus providing model lipid membranes with controlled size and curvature. With fluorescence recovery after photobleaching (FRAP), we observed that droplet-attached lipids, NeutrAvidin proteins, and DNA oligonucleotides all show lateral mobility. A potential application of these droplets with surface-mobile lipids is the self-assembly of colloidal clusters of defined shape. We assembled micron-sized particles on TPM-droplets by either the specific avidin-biotin interaction or by double-stranded short DNA strands, and we conclude that although single linker molecules are mobile, particles that are attached to them are not. We speculate that this is caused by the heterogeneous nature of emulsified TPM, forming an entangled network that limits the collective motion of linkers, but allows mobility of individual TPM-attached molecules.

8.1 Introduction

Interfacial mobility is a distinct property of lipid membranes that is crucial for biological processes in every organism.[11] This property is often isolated in the form of supported lipid monolayers or bilayers, thereby enabling controlled study of processes that involve lipid membranes or membrane proteins.[39,224–226] For example, a recent study has shown that the mobility of antibodies on lipid-coated droplets results in an up to ten times faster uptake by macrophages compared to particles with immobilized antibodies.[227] Next to this, micrometer-sized self-assembly has been inspired by the inherent mobility of lipid monolayers: lipid-coated emulsion droplets have lead to for instance force measurements on cell-cell adhesion,[228] and lipid-coated silica particles to flexible colloidal joints.[44]

We here focus on so-called droplet interface monolayers, which are oil droplets with lipids on their surface.[229] Control over the size of the droplets is important for the involved applications and therefore we here investigate membranes that are supported on 3-(trimethoxysilyl)propyl methacrylate (TPM), which is a polymerizable oil that spontaneously forms emulsions of accurate sizes in between 0.45–4 μm (see Chapter 7). First, we will investigate the mobility of TPM-attached lipids, proteins, and DNA oligonucleotides, which is a key property for both biological studies and self-assembly applications. The resulting lipid-coated droplets mimic biological lipid membranes with controlled size and curvature. Then, we will investigate the use of these TPM-droplet supported lipid monolayers for the bulk production of colloidal clusters.

Clusters of micron-sized spheres are important building blocks in the area of micron-sized self-assembly.[40,230] In order to access their self-assembled structures, multiple methods to prepare colloidal clusters have been developed in the past.[41,43,71] One approach to prepare colloidal clusters is through the assembly of colloidal particles around a central particle. For small cluster sizes, the cluster size and shape is then determined uniquely by the ratio of the particle diameters.[231] Assembly of these optimally packed clusters, however, requires the particles to be able to rearrange over the surface of the central particle.[232] Because the liquid nature of TPM droplets presumably allows for this rearrangement, and the droplet size can be accurately controlled (see Chapter 7), lipid-coated TPM droplets are promising candidates for this application. Therefore, we here investigate the mobility of colloidal particles linked to to the surface of TPM droplets via lipid molecules.

8.2 Methods

Materials 3-(Trimethoxysilyl)propyl methacrylate (TPM, 98 %), ammonium hydroxide (28 %), azobisisobutyronitrile (AIBN, ≥98 %), ethanol (99.8 %), and sodium phosphate dibasic were purchased from Sigma-Aldrich; Sodium chloride (NaCl) and sodium

azide (NaN_3, 99 %) from Acros Organics; DNA oligonucleotides from Integrated DNA Technologies; NeutrAvidin and NeutrAvidin–Oregon 488 from Thermo Scientific; Δ9-cis 1,2-dioleoyl-*sn*-glycero-3-phosphocholine (DOPC), 1,2-dioleoyl-*sn*-glycero-3-phosphoethanolamine-N-[methoxy(polyethylene glycol)-3000] (DOPE–PEG3000), DOPE–PEG2000, DOPE–PEG5000, 1,2-distearyl-*sn*-glycero-3-phosphoethanolamineN[biotinyl-(polyethylene glycol)-2000] (DSPE–PEG–btn), and 1,2-dioleoyl-*sn*-glycero-3-phosphoethanolamine-N-(7-nitro-2-1,3-benzoxadiazol-4-yl) (DOPE–NBD) from Avanti Polar Lipids. All chemicals were used as received. All solutions were prepared from deionized water with 18.2 MΩ cm resistivity, using a Millipore Filtration System (Milli-Q Gradient A10). Phosphate buffered saline (PBS) solution consisted of 25 mM sodium phosphate, 100 mM sodium chloride, and 3 mM sodium azide, in water with the pH brought to 7.5.

DNA oligonucleotides The following DNA oligonucleotides were used:

- Biotin–TEG–3'–TTT TAG CGA TGG GAA GCG TGT CAG TTA GAT CTC TCG GGA CGG AAT GC–5' (btn–B)
- Cy3–5'–TTT ATC GCT ACC CTT CGC ACA GTC AAT CTA GAG AGC CCT GCC TTA CGA *CCT ACT TCT AC*–3' (Cy3–B'–S)
- 6FAM–5'–TTT ATC GCT ACC CTT CGC ACA GTC AAT CTA GAG AGC CCT GCC TTA CGA *GTA GAA GTA GG*–3' (6FAM–B'–S')

Here, A stands for Adenine, C for Cytosine, G for Guanine, T for Thymine, B for base strand, S for sticky end (corresponding bases are printed in italics), TEG for tetraethyleneglycol, Cy3 for a cyanine dye (exc. 550 nm em. 570 nm) and 6FAM for 6-carboxyfluorescein (exc. 495 nm em. 517 nm). These DNA strands were hybridized into double-stranded (ds) DNA, by heating 0.4 nmol Cy3–B'–S/6FAM–B'–S' and 0.8 nmol btn–B to 90 °C in 200 µL PBS. This solution was cooled down to room temperature over the course of 2 h after which the resulting hybridized DNA was stored at 4 °C. In the remainder of this chapter, we use dsDNA–Cy3 as a shorthand for the combination of btn–B and Cy3–B'–S, and dsDNA–6FAM for the combination of btn–B and 6FAM–B'–S'.

TPM emulsification TPM oil was emulsified following the protocol in Chapter 7. In short, 250 µL of 2.8 vol % ammonia was added to 15 mL water in a plastic (PP) beaker covered with Parafilm. The pH was confirmed to be in the range 10.4–10.6 with a Hach H270G ISFET pH probe. While magnetically stirring at 350 rpm, 75–100 µL TPM was injected. After 15 min, the stirring speed was reduced to 200 rpm, and after 2.5 h, the stirring was stopped and the resulting emulsion was stored in a glass vial. For each reaction batch, the dry weight and droplet radius were determined. Using the density of TPM emulsion droplets (1.235 ± 0.010 g cm^{-3}, see Chapter 7), the total TPM/water interfacial area could be computed per volume, which we did for every TPM emulsion. This was then used to compute the 'maximum surface coverage' (MSC), which we here define as the the number of added molecules per TPM/water surface area.

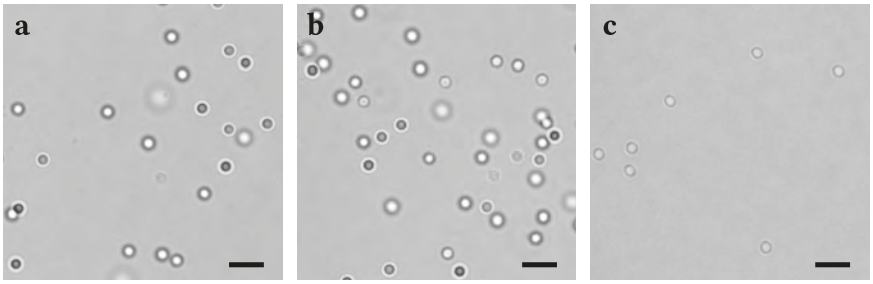

Figure 8.1. Light microscopy images of the same TPM droplets in (a) water, (b) 10 vol % ethanol, and (c) 0.2 vol % isopropanol. The ethanol had no observable effect on the droplets, while the isopropanol clearly reduced the total number of droplets through droplet coalescence and droplet loss at the container walls. Scalebars denote 5 µm.

Lipid transfer Lipids were transferred to the TPM droplets by dissolving the DOPC, DOPE–PEG, and DSPE–PEG–btn in ethanol at 1 g L^{-1}, and then adding them to the TPM droplets in the desired quantity (see Table 8.1). In a separate experiment, we confirmed that the added ethanol did not influence the size of the TPM droplets, while for instance the addition of isopropanol did lead to droplet coalescence and droplet loss at the container walls (see Fig. 8.1). The samples were rotated for at least 3 h in a Stuart Rotator SB3, and then washed two times with water by centrifugation at 43 rcf for 30 min. The lipid-coated emulsion droplets were stored at 4 °C.

Droplet functionalization We functionalized the TPM droplets with NeutrAvidin by adding the desired MSC of NeutrAvidin (dissolved at 1 g L^{-1} in PBS buffer) to lipid-coated TPM droplets. The DNA-functionalization was done by adding a pre-assembled dsDNA—NeutrAvidin construct, which was prepared as follows: NeutrAvidin and dsDNA–Cy3 were mixed in the desired molar ratio (see Table 8.1) in the rotator for a minimum of 3 h. The resulting dsDNA—NeutrAvidin constructs were stored at 4 °C. Then, a lipid-coated TPM emulsion was transferred to PBS and the dsDNA—NeutrAvidin constructs were added up to the desired MSC. The functionalized emulsion was washed three times with PBS. We noted that the presence of the polymer surfactant Pluronic F-127 removed the DNA oligonucleotides from the droplet surface, therefore we recommend avoiding the use of amphiphilic polymers.

We also noted that centrifugation of the coated droplets in PBS lead to partial droplet coalescence and loss at the walls of the sample container. This was solved by avoiding the centrifugation of TPM droplets in PBS. Although we did not use this protocol for the results in this chapter, we provide it here for future reference. First, we added an excess of NeutrAvidin to the emulsion droplets (MSC of 1×10^5 µm^{-1}). After rotating for 3 h, we washed the emulsion two times with water, and re-suspended it in PBS in the last step. Finally, we added the desired amount of DNA.

Table 8.1. Employed TPM droplet functionalization concentrations. All numbers are max surface coverage (MSC) values, given in number of added molecules per μm^2 of water/TPM interfacial area.

#	DOPE–PEG3000 [μm^{-2}]	DSPE–PEG–btn [μm^{-2}]	NeutrAvidin [μm^{-2}]	dsDNA-Cy3 [μm^{-2}]
1	3×10^5	3×10^4	$4 \times 10^{4*}$	-
2	1×10^5	1×10^4	1×10^4	3×10^4
3	-	1×10^6	-	-
4	-	2×10^6	-	-
5	$3 \times 10^{6\dagger}$	-	-	-
6	2×10^5	3×10^4	4×10^4	4×10^3
7	7×10^5	8×10^4	8×10^3	2×10^4
8	2×10^5	3×10^4	8×10^2	8×10^2
9	$8 \times 10^{5\ddagger}$	9×10^4	5×10^3	2×10^3

* NeutrAvidin–Oregon 488 was used instead of NeutrAvidin.

† DOPE–PEG2000 was used instead of DOPE–PEG3000.

‡ DOPE–PEG5000 was used instead of DOPE–PEG3000.

Particle preparation NeutrAvidin and poly(ethylene)glycol coated polystyrene particles with a diameter of 0.98 ± 0.03 µm were prepared using 3.3 µg NeutrAvidin per mg particles following a method described in Chapter 4. For the dsDNA-functionalized particles, these NeutrAvidin-coated particles were incubated for 30 min at 55 °C with the desired amount of dsDNA–6FAM (typically 4×10^3 μm^{-2}) in a PBS buffer, and washed three times with PBS afterwards.

Cluster preparation For the preparation of particle-droplet clusters, particles and droplets were mixed in an estimated 4:1 number ratio at a TPM droplet number density of 10^8 cm^{-3}. The resulting sample was left overnight in the tumbler. For the polymerized sample in Figure 8.3c, clusters were polymerized for 2.5 h at 80 °C with 1 g/L AIBN. In this process, a large fraction of the clusters disassembled, likely due to the unbinding of biotin-NeutrAvidin at elevated temperatures. This might be improved in the future by using a photo-initiator instead of a thermal initiator (see Chapter 7).

Imaging Imaging was done using a Nikon Ti-E A1R confocal microscope equipped with a 100× NA 1.49 oil immersion objective. The Cy3 dye was excited by a 561 nm laser, and the Oregon 488 and 6FAM dyes with a 488 nm laser. Emissions were recorded respectively through 525 ± 25 nm and 595 ± 30 nm filters. The imaging coverslips were pre-treated with a layer of polyacrylamide to prevent droplet adhesion, using the method described in Chapter 5.

FRAP Fluorescence recovery after photobleaching (FRAP) experiments were performed on untreated glass coverslips to fixate the droplets. Using a focussed laser and a set of Galvano mirrors, dye molecules in a region on a single emulsion droplet were bleached, after which we observed the recovery with confocal microscopy. The recovery of fluorescence is caused by the diffusive exchange of molecules from the bleached patch with the rest of the droplet. Following ref. [233], we define the bleaching-corrected relative intensity $I_r(t) = I(t)/I(t = 0)$, with I the bleaching-corrected intensity $I = I_{FRAP}/I_{ref}$. I_{ref} is the fluorescence in a reference area, that captures the global bleaching due to imaging. We then fit $I_r(t)$ to an exponential recovery curve: $I_r = \alpha(1 - \exp[-(t - t_0)/\tau])$, with t the time, t_0 the starting time, τ the recovery time, and α the extent of recovery.

8.3 Results and Discussion

8.3.1 Mobility

The most important property of a droplet-supported lipid monolayer is its mobility. We studied the mobility of single TPM-droplet attached molecules using FRAP. First, we prepared TPM droplets with attached DOPE lipids that have a covalently attached fluorescent dye (DOPE–NBD with an MSC of $1 \times 10^5\ \mu m^{-2}$). The corresponding FRAP experiment (see Figs. 8.2a–d) showed a complete recovery with a recovery time of 0.6 s. The small bleaching area and spherical particle geometry prohibited the quantitative comparison of the timescale with the lipid diffusion coefficients, such as usual for planar supported bilayers.[233] Qualitatively, the order of magnitude of the recovery time in a patch size of approximately 1 µm is comparable to typical diffusion coefficients of DOPE lipids ($10\ \mu m^2\ s^{-1}$, see ref. [234]). From this, we conclude that lipids on TPM microemulsion droplets have a mobility comparable to lipids in a lipid bilayer.

Next, we prepared DOPE–PEG3000/DSPE–PEG2000–btn stabilised TPM emulsion droplets (experiment #1 in Table 8.1) and attached an excess of NeutrAvidin functionalized with the fluorescent dye Oregon 488. See Figs. 8.2e–h for the corresponding FRAP experiment. The observed recovery time of 0.4 s was comparable to the lipid recovery time, so we conclude that TPM microemulsions can be coated with NeutrAvidin proteins that are mobile on the droplet surface. These NeutrAvidin proteins are widely employed to link molecules non-covalently together, which could be used to for instance attach monoclonal antibodies[142,227] or DNA oligonucleotides[48,235] to the liquid droplet surface.

To prove the lateral mobility of NeutrAvidin-attached molecules, we linked double-stranded DNA oligonucleotides to the DSPE–PEG2000–btn—NeutrAvidin construct (experiment #2 in Table 8.1). The here employed dsDNA–Cy3 was functionalized with a fluorescent dye, so that we could use FRAP to quantify the mobility on six particles distributed over two TPM emulsion batches. See Figs. 8.2j–m for a representative result. All droplets showed mobility, with an extent of recovery of 93 ± 2 % and a recovery time of 1.8 ± 0.2 s, which is significantly slower than the recovery of the NeutrAvidin proteins. We presume this is related to the size of the double-stranded DNA.

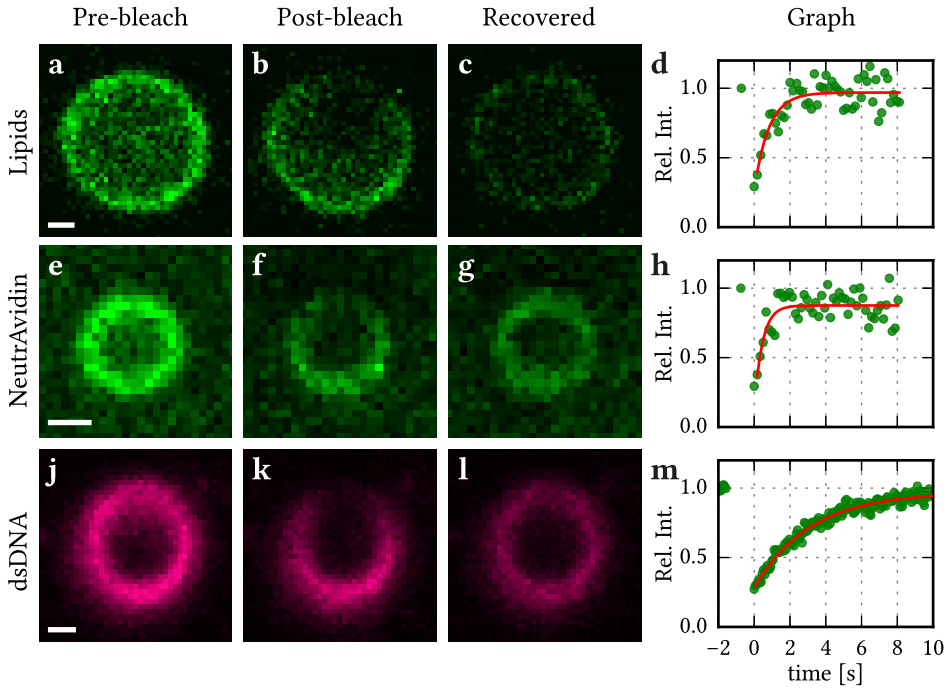

Figure 8.2. FRAP experiment showing the mobility of molecules attached to TPM emulsion droplets. In (a) to (d), confocal images of DOPE–NBD (experiment #1 in Table 8.1) on the surface of a TPM droplet are shown (a) before bleaching, (b) directly after bleaching, and (c) after recovery. In (d), the bleaching-corrected relative intensity is shown, together with a least squares fit with recovery time 0.6 s. The relative intensity is subject to error in the first (pre-bleach) data point. Within this error, the observed recovery was complete. Similarly, in (e) to (h) the recovery of NeutrAvidin–Oregon 488 (experiment #2 in Table 8.1) is shown with recovery time 0.4 s. In (j)–(m) the recovery of dsDNA–Cy3 (experiment #3 in Table 8.1) is shown with recovery time 1.8 ± 0.2 s and relative recovery of 93 ± 2 %. The videos corresponding to these three FRAP experiments are available online.

These results show that lipid-coated TPM droplets can be functionalized with surface-mobile macromolecules, which provides a versatile platform for in vitro biological studies such as phagocytosis.[227]

8.3.2 Cluster self-assembly

As alluded to in the introduction, droplets with surface-mobile molecules are promising candidates for applications in micron-scale self-assembly. The preparation of TPM droplets with linked colloidal particles that are able to rearrange on the TPM surface

would open up a way to bulk synthesize colloidal clusters of well defined shape.[231,232] Also, these flexible TPM-based clusters could be used as microscopic equivalents to hinges and joints, as has been shown recently using lipid bilayer-coated silica microparticles.[44] We here investigate two types of linkages between lipid-coated TPM droplets and particles to obtain these flexible clusters: biotin-NeutrAvidin (as described in Chapters 4–6) and complementary DNA oligonucleotides.[41,44,119]

Starting from DSPE–PEG–btn coated TPM droplets, we created colloidal clusters by mixing the TPM droplets with NeutrAvidin-coated polystyrene particles (experiment #3 in Table 8.1). Through the specific biotin-NeutrAvidin linkage, the particles accumulate on the TPM droplets and colloidal clusters formed within minutes, as can be seen in Figure 8.3. The NeutrAvidin-coated polystyrene particles attached specifically to the biotin-coated TPM droplets: we did not observe clustering of polystyrene particles or TPM droplets at these conditions. Indeed, in the absence of biotin on the TPM particles (experiment #5 in Table 8.1), NeutrAvidin-coated polystyrene particles did not attach to the TPM droplets. The formed clusters can be fixated by polymerizing the TPM droplet (experiment #4 in Table 8.1), which enables the use of these clusters as building blocks for self-assembly. See Figure 8.3c for a SEM image of a polymerized cluster.

The resulting colloidal clusters were however not of uniform shape. This is caused by the immobility of the particles on the TPM droplet surface, which was confirmed separately by following the relative orientations of the particles in a single cluster. Because we presume that the TPM droplet is liquid, this result is surprising. There is apparently sufficient friction between the TPM and particle to fixate most of the clusters, at least during a single cluster observation of a few minutes. Unlike experiments on a similar system,[44] we here observed that lowering the number of biotin linkers on the TPM droplets did not result in a reproducible cluster flexibility. A probable explanation for this is that the PEG2000 polymers on the TPM droplet have insufficient length (Flory radius of 3.5 nm[136]) to prevent Van der Waals interactions between the TPM oil and polystyrene particles. Therefore, we took another approach and investigated the use of double-stranded DNA 'linkers' (dsDNA) that protrude approx. 14 nm from the TPM droplets. The dsDNA terminates with a single-stranded 'sticky end' that protrudes from the particle, which allows binding with its complementary strand[119] while keeping the bound particle sufficiently far from the TPM surface to prevent Van der Waals forces to fixate the cluster.

The specific interactions between DNA oligonucleotides only function in the presence of salt. As the salt screens the electrostatic repulsions between TPM droplets, additional stabilization of the TPM droplets is necessary to prevent droplet coalescence. We achieve this by coating the particles with an excess of DOPE–PEG3000. With a concentration series, we observed that a minimum MSC of $6 \times 10^4\ \mu m^{-2}$ is necessary to prevent droplet coalescence in 0.1 M NaCl. Note that this MSC is the number of added lipids to the TPM emulsion, and not the actual number of lipids per unit area, which presumably is lower. The thus stabilised TPM-droplets can be easily centrifuged and are stable for weeks in the tumbler.

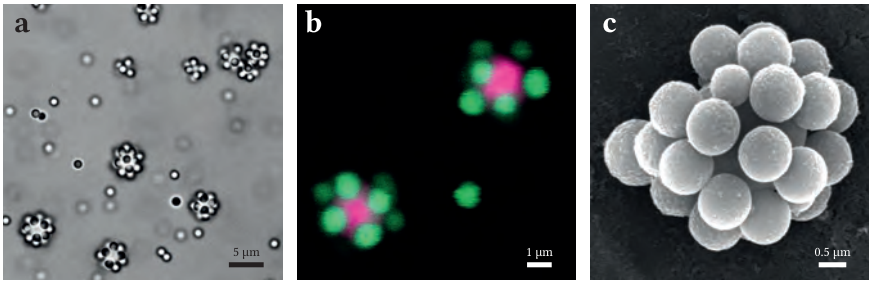

Figure 8.3. Colloidal clusters from DSPE–PEG2000–btn coated TPM droplets and NeutrAvidin-coated polystyrene, in water. (a) Bright field image of several colloidal clusters and free polystyrene (experiment #3 in Table 8.1). (b) Confocal image of the same sample with two TPM droplets (magenta) each surrounded by multiple attached polystyrene particles (green). (c) Scanning electron micrograph (taken by an FEI NanoSEM) of a TPM droplet with attached polystyrene particles, that was polymerized after cluster assembly (experiment #4 in Table 8.1).

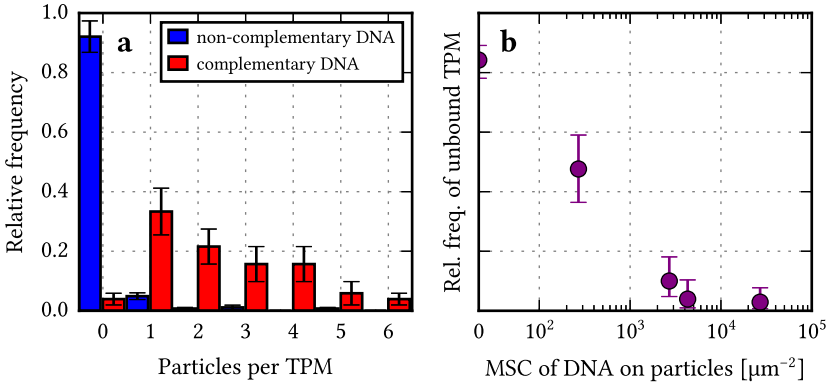

Figure 8.4. DNA-mediated cluster formation of TPM droplets with polystyrene particles (see experiment #6 in Table 8.1). (a) Distribution of cluster sizes for dsDNA–Cy3 coated TPM droplets with complementary particles (dsDNA–6FAM coated) and non-complementary particles (dsDNA–Cy3 coated). After 3 h, 98% of the TPM droplets have bound to at least one complementary particle, while only 8% of the droplets bound to the non-complementary particles. The droplet:particle number ratio in these experiments were 1:2.3 and 1:0.7, respectively, and the MSC of DNA on the particles was 4.3×10^3 µm^{-2}. (b) The probability of observing unbound TPM droplets increased with decreasing DNA coverage on the particles. This provides additional evidence that DNA is causing the droplet-particle binding.

On these stabilised TPM droplets, we assembled NeutrAvidin—dsDNA–Cy3 constructs, which can be visualised through the fluorescent dye Cy3 on the DNA, see Fig. 8.2j. To prove the specific assembly o0.f particles on these TPM droplets, we then added particles with the complementary (dsDNA–6FAM) DNA strands and particles with the non-complementary (dsDNA–Cy3) DNA strands (see experiment #6 in Table 8.1). After 3 h we counted the formed clusters and observed that in the first case, 98% of the TPM droplets was indeed bound to at least one particle, as opposed to 8 % in the control experiment (see Fig. 8.4a). The probability of binding increased with increasing DNA density on the polystyrene particles, as displayed in Fig. 8.4b. We therefore concluded that the observed binding is due to the complementary DNA strands.

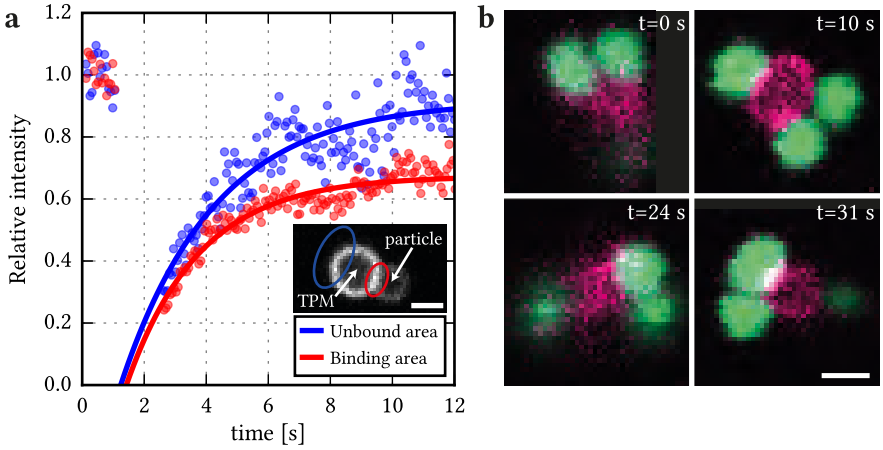

Figure 8.5. The mobility of DNA-mediated TPM clusters. (a) The FRAP recovery of dsDNA linkers in the binding area is only 67% (red), as opposed to the 92% recovery in an unbound area (blue). The corresponding confocal image is displayed in the inset, together with the approximate FRAP areas of the binding patch (red) and unbound area (blue) (experiment #7 in Table 8.1). (b) Four confocal images of the same DNA-mediated TPM cluster (experiment #8 in Table 8.1). The cluster rotation is visible, however the relative orientation of particles remains fixed. Clusters with fixed conformations were observed throughout all samples. The corresponding video is available online. Scalebars denote 1 µm.

The DNA-mediated linkage between TPM droplets and polystyrene particles can also be observed in a FRAP experiment (experiment #7 in Table 8.1). In Figure 8.5a, the recovery of DNA fluorescence in a binding area is compared to the recovery outside the binding area. The bleaching-corrected fluorescence in the binding area was observed to recover to only 67% after photobleaching, while the unbound area recovered to 92%. This incomplete recovery shows that part of the DNA linkers are confined inside the linking patch between the TPM droplet and polystyrene particle, which is a logical consequence of the DNA-mediated linkage between droplet and particle.

Although we concluded that the DNA linkages were mobile on the TPM surface with the droplet-particle linkage caused by the DNA, we did not observe mobility of the particles on the TPM droplets. This is illustrated in Figure 8.5b, in which the relative orientation of the polystyrene particles on the central TPM droplet does not change over the course of the experiment (1 min). One factor that may influence the cluster flexibility is the number of particle-droplet linkages. In similar work[44] that uses lipid bilayer-coated silica particles to form colloidal clusters, it was found that mobile clusters are found only below a DNA surface concentration of $1 \times 10^4\ \mu m^{-2}$. However, we observed that at a DNA maximum surface coverage (MSC) of $2.7 \times 10^2\ \mu m^{-2}$ on the particles, the clusters were still not flexible. Because at this coverage, almost half of the TPM droplets does not bind any particle (see Fig. 8.4b), we conclude that we cannot achieve mobile clusters by reducing the number of DNA linkages.

We here propose two possible reasons for the lack of cluster mobility. Firstly, the steric stabilization of the TPM droplets might be insufficient. We attempted to improve the thickness of the steric stabilization layer by using DOPE–PEG5000 lipids instead of DOPE–PEG3000 (see Table 8.1, experiment #9), however this also did not lead to mobile clusters. Therefore, we suggest a second reason for the absence of cluster flexibility, which is connected to the heterogeneous nature of TPM. The TPM microemulsion droplets are formed by hydrolysis and subsequent oligomerization of TPM monomers (see Chapter 7). It is likely that TPM oligomers are predominantly present on the TPM droplet surface and form a network of crosslinked TPM molecules. Single molecules that are embedded in this interface are able to move on this heterogeneous surface, while collective motion of multiple linkages is prohibited. See Figure 8.6 for an illustration of this hypothesis. This would explain the almost complete recovery of dsDNA on the TPM

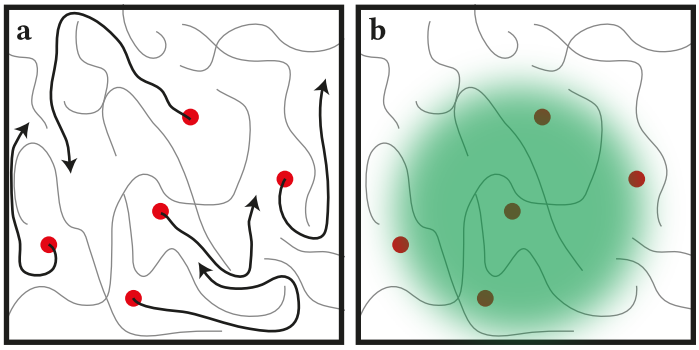

Figure 8.6. Sketch illustrating the hypothesized effect of TPM heterogeneity on the collective mobility of attached lipid molecules. (a) Single lipid molecules (red discs) can freely move through the network of TPM oligomers (grey lines), as denoted with the black arrows. (b) If the same lipids would be interconnected by a linked particle (green shaded area), they move collectively, and their movement becomes inhibited by the TPM oligomer network.

droplet surface (see Fig. 8.2), and at the same time the immobility of clusters that are formed exclusively through dsDNA linkages.

8.4 Conclusion

We have shown that TPM droplet surfaces can be used as a lipid monolayer support. Using fluorescence recovery after photobleaching, we have proven that the fluorescence provided by DOPE-NBD lipids on the interface of TPM droplets fully recovers within seconds after photobleaching, which is comparable to lipid diffusion in bilayers. Also, when the protein NeutrAvidin is attached to a DOPE-PEG2000-btn lipid, an equally high mobility was observed. Using remaining binding sites on the NeutrAvidin, we attached double-stranded DNA oligomers, which also showed lateral mobility, albeit with a longer recovery time of 1.8 ± 0.2 s and with a recovery after photobleaching of 93 ± 2 %. TPM microemulsions therefore provide a model of cells with surface-mobile moieties, which will be useful in the future for controlled phagocytosis experiments.[227]

Because TPM droplets can be produced with a narrow size distribution, these are interesting candidates for the self-assembly of micron-sized colloidal clusters. We showed that NeutrAvidin-coated particles attach to biotin-coated TPM-droplets, and also that the resulting clusters could be fixated by polymerizing the TPM droplets, enabling their use in further self-assembly steps. Using a different approach with double-stranded DNA oligomers, we were also able to specifically assemble particles on the surface of TPM droplets.

Surprisingly, the resulting clusters were not flexible, while we established that the single molecules that link the droplet and particles together are mobile on the TPM surface. We hypothesize that the mobility of a collection of TPM-attached molecules is inhibited because of the oligomeric TPM structures that are present in the TPM droplets. While most of the single linkers are able to diffuse through this network of TPM oligomers, a collection of linkers is effectively stuck at a fixed position on the TPM droplet. TPM droplets thus provide an interesting mixture of single lipid mobility and collective immobility, which will be interesting for further research.